CONDUCTANCE IN NANOWIRES

H. MEHREZ AND S. CIRACI

Department of Physics,
Bilkent University,
06533, Ankara, Turkey

Abstract. This paper presents a detailed analysis of conductance and atomic structure in metal nanowires under tensile stress. We calculate the variation of conductance with the crossection of the constriction between two reservoirs, that is represented by three-dimensional circularly symmetric potentials. The absence of several observed features in the calculated conductance variations, in particular sudden jumps, suggests that the discontinuous rearrangements of atoms under stretch dominate the electron transport. To analyze the variations of atomic structure, we performed simulations based on the state of the art molecular dynamics simulations and revealed novel structural transformations. It is found that yielding and fracture mechanisms depend on the geometry, size, atomic arrangement and temperature. The elongation under uniaxial stress is realized by consecutive quasi elastic and yielding stages; the neck develops mainly by the implementation of a layer with a smaller crossection at certain stages of elongation. This causes to an abrupt decrease of the tensile force. Owing to the excessive strain at the neck, the original structure and atomic registry are modified; atoms show tendency to rearrange in closed-packed structures. In certain circumstances, a bundle of atomic chains or single atomic chain forms as a result of transition from the hallow site to the top site registry shortly before the break. The origin of the observed "giant" yield strength is explained by using results of present simulations and *ab initio* calculations of total energy and Young's modulus for an infinite atomic chain.

G. Abstreiter et al. (eds.), Optical Spectroscopy of Low Dimensional Semiconductors, 213–234.

1. Introduction

The optical, electronic and mechanical properties of condensed systems with nanometer dimensions can be rather different from those of the bulk. The effects of reduced size and dimensionality, in particular properties leading to novel devices have been subject matter of several research works in the last decade[1]. By pulling the tip of a scanning tunneling microscope (STM) after the nanoindentation[2-6] or by bending a mechanically controllable break junction[7], long metal wires with diameters in the range of few λ_F have been produced. As the crossection of the wire is reduced by stretching it continuously, the two terminal conductance G is measured. The measured conductance showed irregular and sudden changes with stretch s; the detailed behavior of which was not only sample specific, but also was varying in different scans of the same experiment. The abrupt falls of $G(s)$ became generally sharper and closer to the integer multiples of quantum conductance ($G_o = 2e^2/h$ per two spin) with decreasing crossection prior to the break of the neck. This has been taken as a manifestation of the quantization of conductance in atomic size wires (or connective necks). In contrast to various quantization arguments[5,6], some authors related abrupt variation of $G(s)$ to the irregular and discontinuous changes of the crossection of the wire $A(s)$ in the course of stretch[8-11]. Presently, these predictions were strengthened by the experimental results[12,13] that have been obtained by using a combination of STM and AFM (atomic force microscope). These experiments have shown that any sudden change in conductance is accompanied by an abrupt modification of atomic structure and hence the crossection of the neck. The yield strength σ_Y measured shortly before the break has been found much higher than that of the bulk.

The narrowest diameter of the nanowire prior to the break is only a few angstrom; it has the length scale λ_F, where discontinuous (discrete) nature of the metal dominates over its continuum description. For example, in this length scale, the level spacings of electrons $(0.1 - 1eV)$ become easily resolved even at room temperature, and any change of atomic structure may lead to detectable changes in the related properties. For example the ballistic electron transport through nanowire is expected to be closely related with the atomic structure at the narrowest part of the connective neck. It becomes now clear that the mechanical properties, in particular the yielding mechanisms of the nanowires are quite different from those of bulk material.
We believe that the subject of dispute about the quantization of conductance emerges from the diverse criteria; this will be clarified in the present work by the analysis of ballistic transport in a nanoindentation and in an atomic size connective neck that is pulled between two electrodes. In this

paper, we investigate the ballistic electron transport on the idealized wires which have circularly symmetric potential but short necks as in the experiment. Since the calculated variation of G with the radius does not exhibit sharp step structure, we seek the origin of the abrupt jumps in the structural changes of the wire during stretch. To this end, we carry out state of the art Molecular Dynamics (MD) studies which indicate a clear connection between the strain induced atomic rearrangement and conductance variations. We found novel atomic processes and atomic rearrangements induced by the applied stress. By using these results we provide a consistent interpretation for various structures of G observed in the course of stretch. While the step falls (or jumps) of $G(s)$ are associated with the sudden changes in the crossection, the spikes on the plateaus may be due to transient motion (migration) of atoms in the narrowest region of the neck or resonant tunneling through the constriction. The positive slope observed on the last plateau of Pt and Al wires[7] is due to increasing local density of states $\rho(r, E_F)$ at the neck which undergoes a structural transformation under extreme strain.

2. Conductance in the Nanowire

How the conductance of a mesoscopic object depends on its size and dimensionality has always been attractive, as well as intriguing subject for researchers. As early as 1957, Landauer[14] proposed that the conduction in a solid is a scattering event, and that transport is the consequence of the incident current flux. Based on the counting arguments of the transmission T, and reflection R, he derived his famous formula for the conductance $G = (2e^2/h)(T/R)$. Almost three decades ago Sharvin[15] pointed out the resistance of a ballistic channel (or point contact) and developed a formalism in the semiclassical regime. Nowadays, almost defect-free electronic devices have been fabricated, which have dimensions, in one or more directions, on the quantum scale. The two terminal conductance of such a quasi $1D$ device (or constriction) fabricated from the high mobility GaAs-$Al_{1-x}Ga_xAs$ heterojunction[16,17] (which have width w in the range of Fermi wavelength λ_F, and length d smaller than the electron mean free path) were found to change with w approximately in steps of $2e^2/h$. This observation has been interpreted as the quantization of the ballistic conductance. It became clear from subsequent studies[9,18,19] that the motion of electrons in the constriction is transversally quantized if $d \sim \lambda_F$, and then its level spacings become in the range of a few Kelvin, if w is in the range of λ_F. A n-fold degenerate current-carrying state becomes conducting and hence G increases by $2e^2n/h$ whenever its energy coincides with E_F; this situation is denoted as the opening of a n-fold channel. The variation of G

with w displays sharp steps of integer multiples of $2e^2/h$, and flat plateaus form between two consecutive steps provided that the potential in the constriction is uniform, temperature and bias voltage are low, and tunneling contribution is negligible. Otherwise, conduction channels mix significantly, the opening of channels are delayed, sharp step structure is smeared out and step heights are lowered[9].
The atomic size point contact was produced first by the STM: By displacing the tip towards the sample surface, the conductance were measured in a wide range covering tunneling and ballistic regimes. The experimental $logG$ versus tip displacement either exhibits a linear variation and then saturation at the first plateau before a jump, or it ends the linear variation directly by a jump[2].
Theoretical studies[8,20,21] showed that the two terminal conductance at the single atom contact shall be in the range of $2e^2/h$. Furthermore, it has been shown that the observed jumps of conductance originate from the discontinuous and abrupt change of crossection of the contact[8-10].
Better controls of dimensions[4-6] has led to a renewed interest in the transport through the connective necks produced by STM. The principle issue is to what extent the observed structures in the conductance versus stretch curve $G(s)$, comply with the quantization of ballistic conductance. It is expected that the atomic structure of the neck is rather irregular and the potential is nonuniform. The narrowest part of the neck, which determines conductance, is rather short. In those circumstances, the sharp quantization with marginal channel mixing should not occur. Of course the transversal motion of electrons in the neck is quantized with significant level spacing; the effect of this quantization is reflected to the transport. We strengthen our arguments by performing calculations of conductance for uniform constrictions, where the channel mixing shall be insignificant. We will show that the features of $G(s)$ or $G(A)$ for these idealized wires are rather different from the observed behavior.

3. Ballistic Free Electron Model

The nanowire which is connected to the left (L) and right (R) reservoirs (or metal electrodes) by a neck is viewed as a constriction represented by a $3D$ confining potential $V(\vec{r})$. A free electron of the L-reservoir with wave function Ψ_i, enters in the constriction with a finite momentum in the $z-$direction and evolves into current-carrying states[9]. These current-carrying states, either propagate to the R-reservoir or are occasionally scattered, and eventually reach the R-reservoir. The current-carrying states inside the constriction are determined by using multiple boundary matching method, and the conductance is calculated by evaluating the current oper-

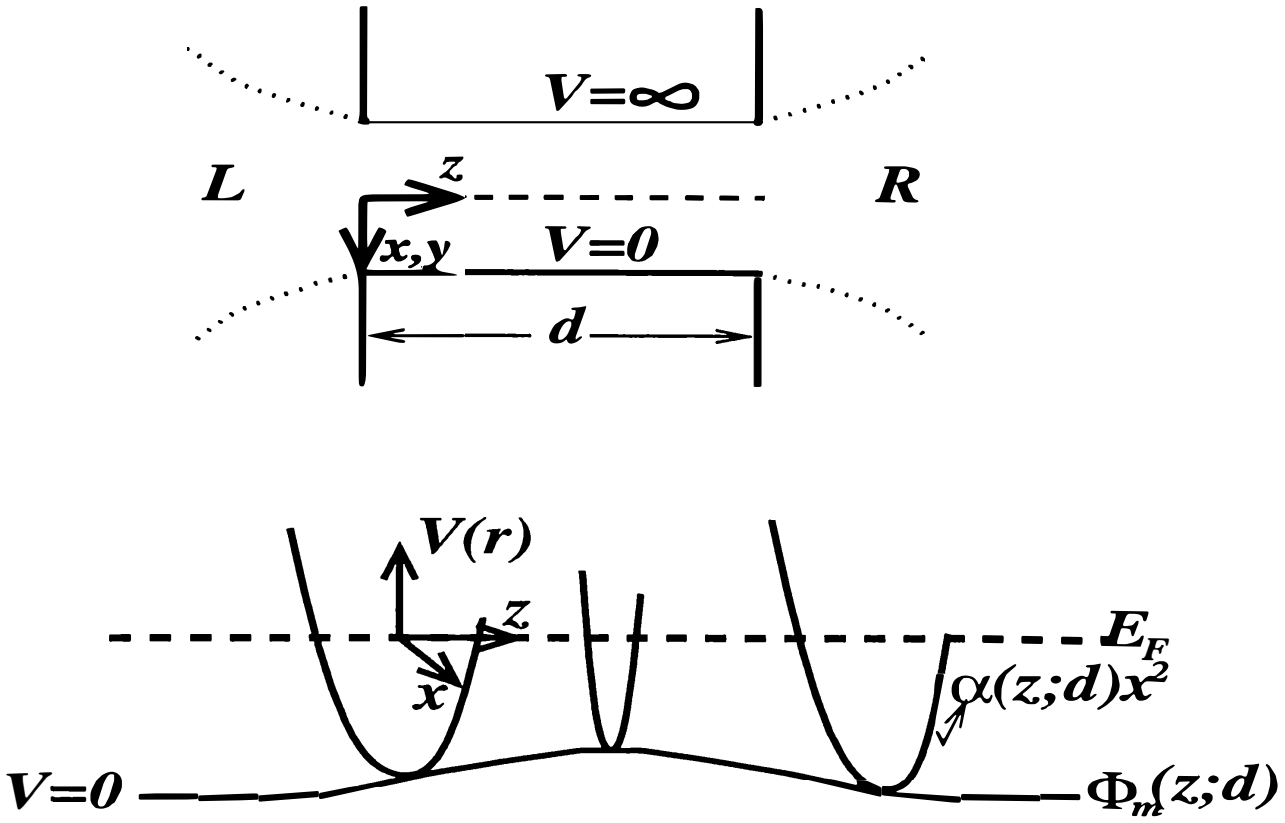

Figure 1. Schematic description of the constriction connected to the left (L) and right (R) reservoirs, which is used to model the electron transport through a nanowire. (a) The infinite wall cylindrical potential with abrupt (continuous line) and trumpet-like (dotted line) connections to the reservoirs. (b) Schematic description of the parabolic potential in the (xz)-plane

ator. As a simplest approximation, the infinite wall cylindrical potential is used for $V(\vec{r})$:

$$\begin{aligned} V(\vec{r}) &= 0 \text{ for } (x^2+y^2)^{1/2} < R(z) \\ V(\vec{r}) &= \infty \text{ otherwise} \end{aligned} \tag{1}$$

Here $R(z)$ is the radius of the constriction which depends on the z coordinate.

Our self-consistent field (SCF) pseudopotential calculations for infinite Al and Na atomic wires with optimized nearest neighbor distance, suggest that the parabolic potential form in the transversal direction is better suited for $V(\vec{r})$. The self-consistent pseudopotential is parameterized as follows:

$$V(\vec{r}) = \Phi_m(z;d) + \alpha(z;d)(x^2+y^2) \tag{2}$$

Here d is the length of the constriction (or neck), and Φ_m is the saddle point potential, which occurs for finite constriction. The two different approximations for the constriction potential are described in Fig.1. We note that these potentials with circular symmetry are very idealized description of the realistic potential inside the constriction. Because of circular

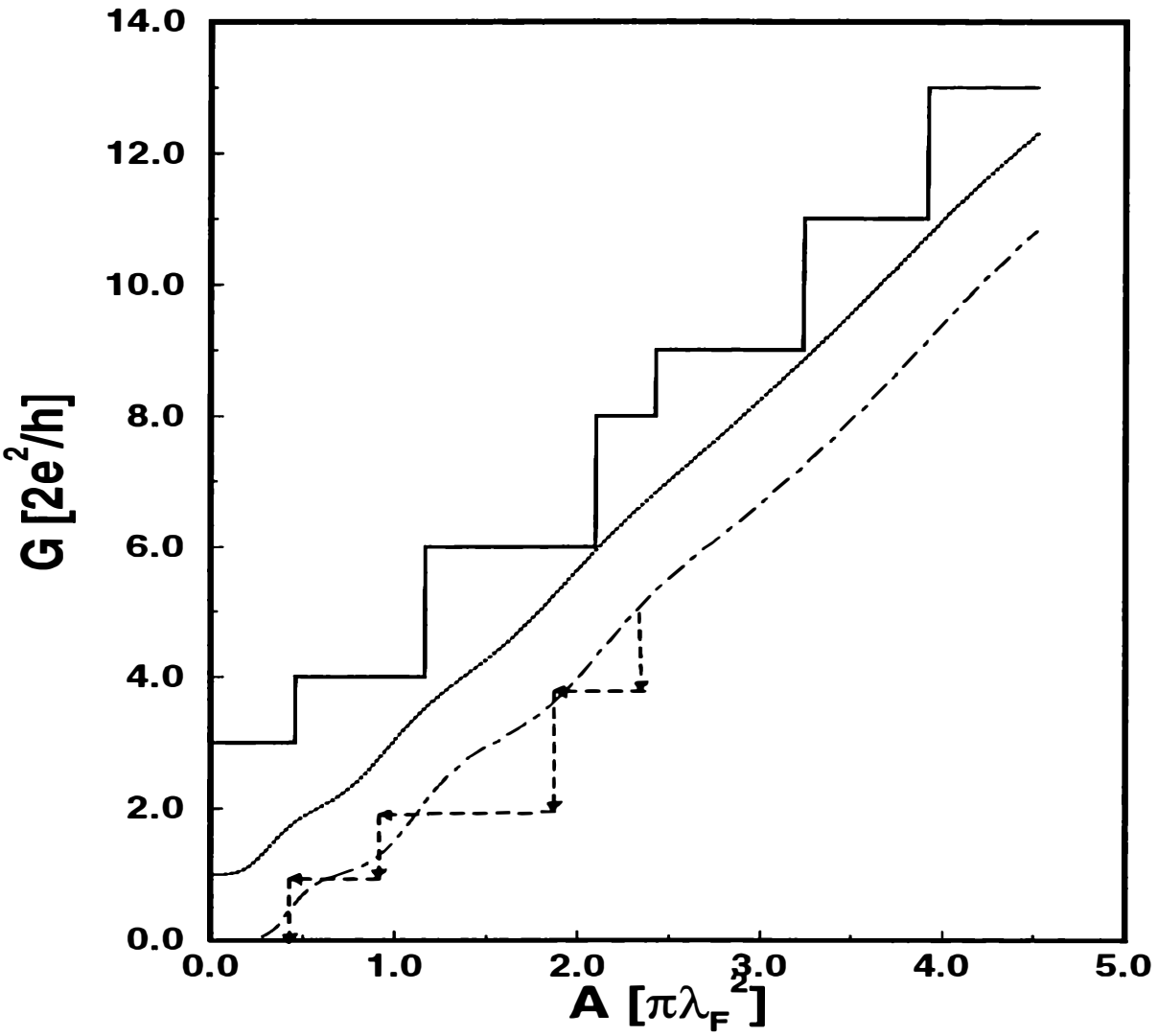

Figure 2. Conductance G versus crossection A for a constriction with an infinite wall cylindrical potential and abrupt connections to reservoirs. Continuous line is for the infinite and uniform neck; dotted line is the quantum Sharvin regime with $d \sim 0$. Uniform and finite neck having $d \sim \lambda_F$ corresponds to dash-dotted line. The discontinuous change of A during stretch give rise to sharp steps as schematically described by dashed lines. The curves are up-shifted for clarity.

symmetry, one can obtain analytical solutions for the wave functions in the transversal $(xy)-$plane. For example, in the parabolic confinement given by Eq.2, the wave functions can be separable in the transversal $(xy)-$plane and in the longitudinal $z-$direction, and the transversal ones become $2D$ harmonic oscillator wave functions.

By using the above forms of the potentials with the abrupt or trumpet-like connections to the reservoirs, we calculate the variation of the conductance as a function of the crossection. By comparing the calculated curves $G(A)$ with the conductance versus stretch curves obtained experimentally, we aim to draw conclusions on the quantization of ballistic conductance in nanowires or connective necks. Figure 2 illustrates our results for G versus crossection A for the infinite wall cylindrical potential with uniform radius R that is connected abruptly to the reservoirs. The dotted curve

corresponds to Sharvin's conductance of a contact with $d \sim 0$. Owing to $d \ll \lambda_F$, the quantization is not completed and step structure is smeared out by tunneling. On the other hand, as $d \to \infty$, the current carrying states have the same quantization at every point along the constriction. Tunneling and mixing of channels do not take place and hence, the variations of G with A displays sharp step structure. Here, any quantized state that coincides with the Fermi level opens a conduction channel and contributes to the ballistic conductance by $2ne^2/h$; n being the degeneracy of the state. In an intermediate situation, i.e $d \sim \lambda_F$, the effect of quantization of transversal state in the neck becomes apparent in the $G(A)$ curve; but neither the steps are sharp nor the the plateaus are flat. Calculations by using uniform parabolic potential with abrupt connections to L- and R-reservoirs and with $d = \lambda_F/2$ and $d = \lambda_F$, lead to essentially the same conclusions.

Next we consider a constriction potential which has abrupt connection from one end and trumpet-like connection from the other end. Such a potential may correspond to the nanoindentation of an STM tip into a flat metal surface. The crossection and the length of the contact can be calculated as a function of the displacement of the tip towards the surface by using continuum contact mechanics or simply by assuming incompressible material in the nanoindentation. Figure 3 shows variation of G with the crossection A and with the push s for different cone angles 2α. We note that the contact made by a tip having relatively larger cone angle, has shorter length d and hence relatively weaker step structure.
Two important approximations are made for the above calculations:
i) Within the continuum approximation, we assumed that the crossection of the neck varies continuously. This may be a reasonable approximation for a metal wire which has large diameter ($2R \gg \lambda_F$). However, as we show in the next section, the crossection of an atomic size wire changes discontinuously.
ii) The potentials we used in calculating G are too idealized and have circular symmetry. The simulation of stretch in the next section show that the crossection of the wire is not circular, and its surface is rather rough.

The constrictions we studied above have weak features in the $G(A)$ curves that are different from the experimental curves. If the structure of experimental $G(A)$ or $G(s)$ is attributed to the quantized conductance the conditions of the above constrictions would be even more suitable for perfect quantization. Apparently, the earlier interpretation of the experimental results have to be revised. In what follows, we show that the discontinuous rearrangement of atoms and structural transformations are essential for a better understanding of the observed $G(s)$ curves.

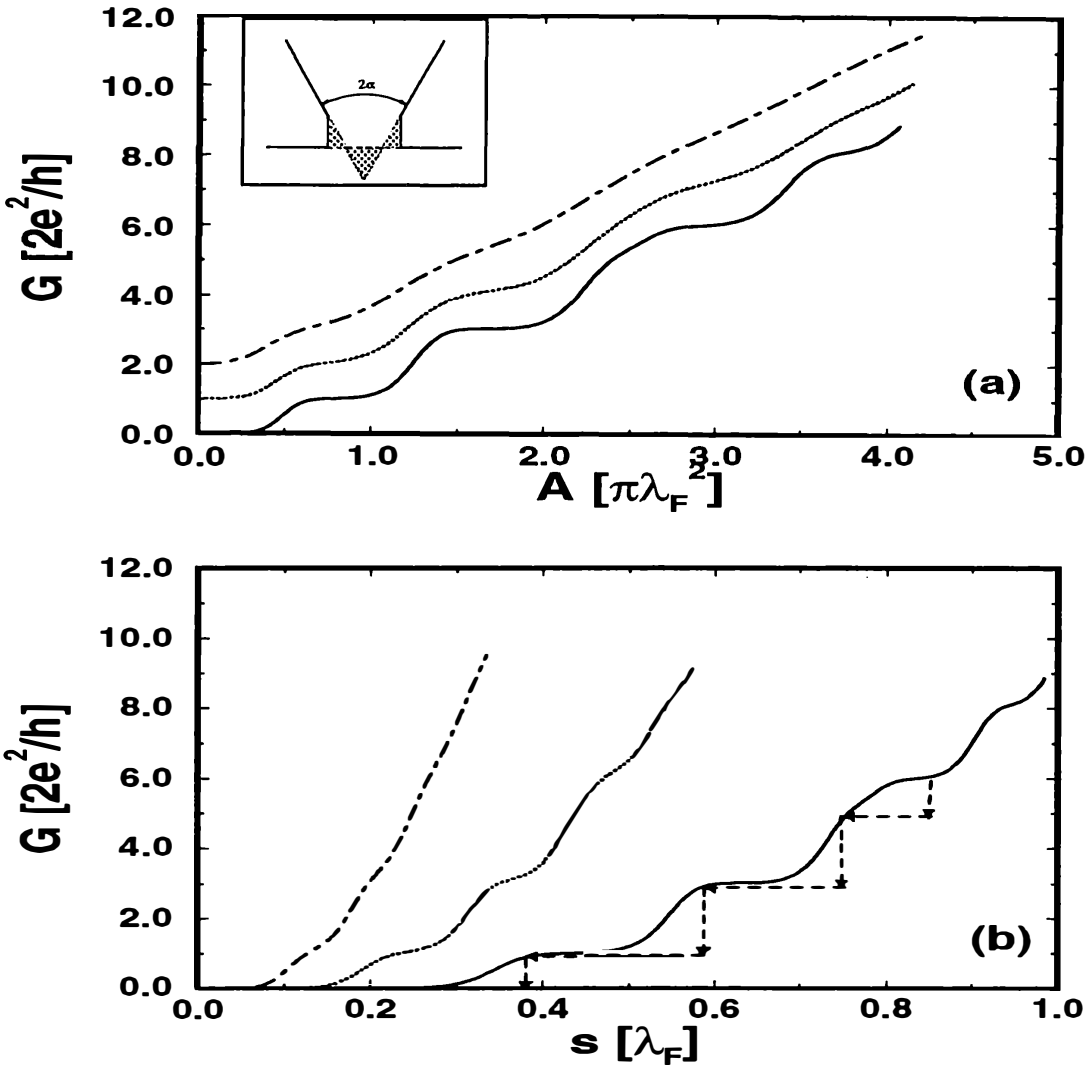

Figure 3. (a) G versus A for a contact formed by an STM tip indenting the substrate surface. (b) same curves plotted as a function of the displacement s of the tip towards sample. Dash-dotted, dotted and continuous curves correspond to the cone angles $2\alpha = 120^o, 90^o$ and 60^o, respectively.

4. MD-Simulations

4.1. DESCRIPTION OF MD-SIMULATIONS

In this section, we study yielding and fracture mechanisms of nanowires that are pulled by an external agent. To understand the origin of these mechanisms and abrupt force variations[12,13], we perform an extensive analysis of atomic structure in the course of pulling. In particular, we follow the motion of the neck atoms and examine their coordination numbers and the structure of atomic layers during the abrupt force variations. We use embedded atom (EA) potential[22-24], and carry out simulations based on the MD method for the Cu nanowires made from (001) and (111) atomic planes[25]. Recently, the MD simulation is proven to be powerful method to

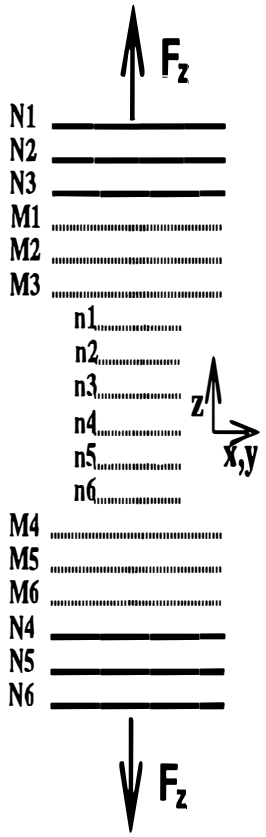

Layer / Wire	N1 N2 N3 N4 N5 N6	M1 M2 M3 M4 M5 M6	n1 n2 n3 n4 n5 n6	Layer Struc.	Poten.
WN1	145 144 145 145 144 145	144 145 144 144 145 145	13 12 13 12 13	Cu(100)	EA
WN2	143 143 143 143 143 143	143 143 143 143 143 143	12 12 13 12 12 13	Cu(111)	EA

Figure 4. Schematic description of the Cu nanowires. The layers labeled by N, M and n are described in the text. The number of atoms in each layer and their $2D$ structure before pulling are indicated. The $x-$ and $y-$axis lie in the atomic [(001) or (111)] planes. The z axis coincides with the axis of the wire; the tensile force $\mathbf{F}_z$ is applied along the z-axis. EA stands for the embedded atom potential.

reveal the atomic rearrangement under tensile stress[3,5,25-27]. The wires we studied have two ends that are connected by a neck, and have quasi-circular crossections. Their structures are summarized in Fig.4. Last three layers at both ends (N_1, N_2, N_3 and N_4, N_5, N_6) are robust: All the atoms in these layers are translated solidly along the stretch direction only by the increment Δl; otherwise they are kept fixed during the MD-steps. These fixed three layers are assumed to be connected to the external agent that applies the tensile stress. Atoms in the following three layers adjacent to the fixed ones (M_1, M_2, M_3 and M_4, M_5, M_6) and those of the neck ($n1, n2, n3...$) are fully relaxed during the MD-steps. The nanowire indicated by $WN1$ is formed from Cu(001) atomic layers. The wire itself is represented by a periodically repeating system in the $(xy)-$plane. The z-axis is taken to be parallel to the axis of the nanowire. $WN2$ is made from Cu(111) atomic planes, and it is investigated at $T = 300K$ and $T = 150K$. The pulling (stretch) is realized by displacing the fixed layers (N's) solidly along the $z-$direction by the increment of length Δl ($0.1\mathring{A}$). After each increment, the atoms of the wires (M's and n's) are relaxed to find their new positions. Simulations are performed with time steps of $0.1ps$ Between two

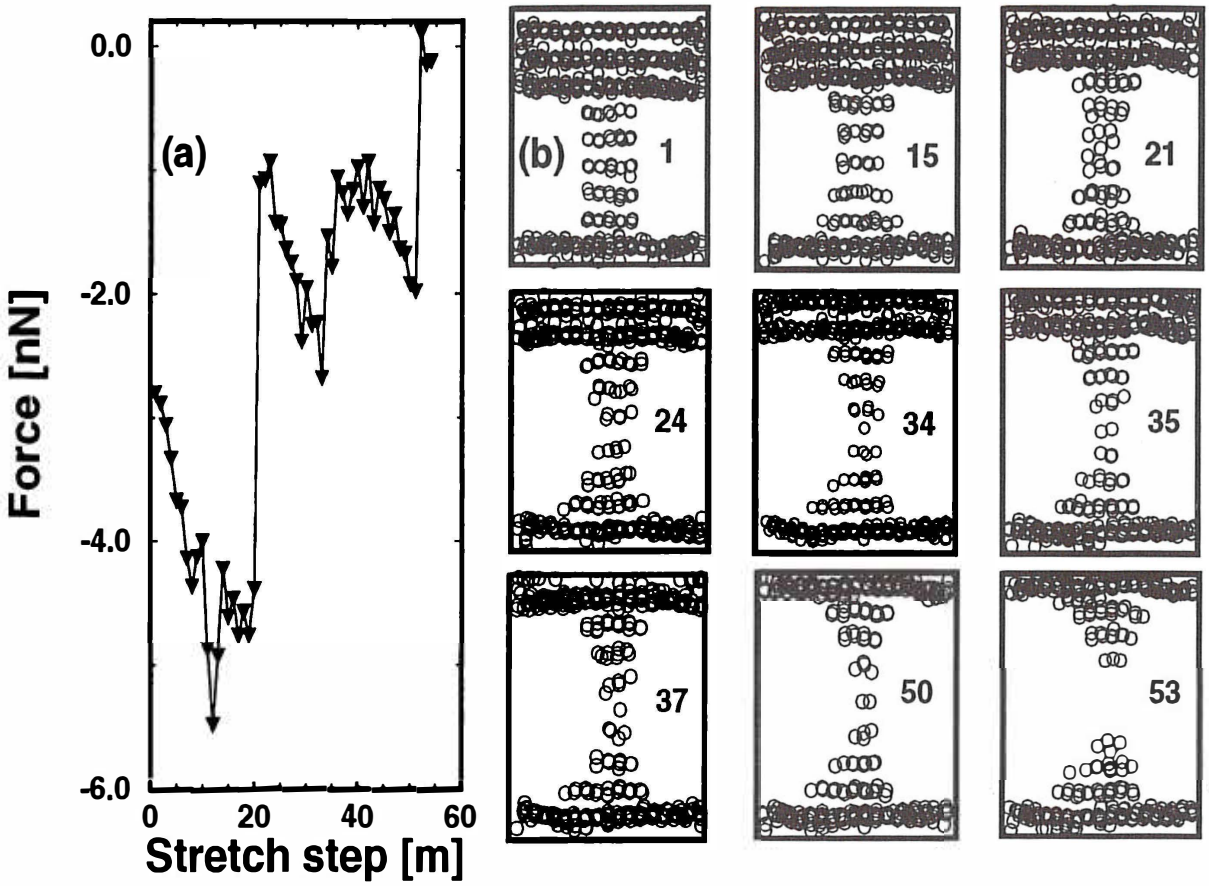

Figure 5. (a) The variation of the force $\mathbf{F}_z$(nN) with the strain or elongation along the z-axis applied by pulling the end layers of Cu (WN1) by $m\Delta l$ at $T = 300K$. (b) The side views of the nanowire showing the atomic positions at some relevant stretch values m.

subsequent stretches of Δl the nanowire is relaxed for $2500ps$. The tensile force $\mathbf{F_z}$ (which is the attractive force between the fixed top three layers and the rest of the wire) is obtained after averaging over the last 800fs, so that the force fluctuations are minimized.

4.2. MD RESULTS FOR Cu(001) NANOWIRE

In this section we examine the elongation and various physical events during the stretch of the nanowire, $WN1$ at $T = 300K$. The initial atomic configuration of the nanowire is described in Fig.4. The interlayer distance between the bulk Cu(001) layers is $c \sim 1.8\mathring{A}$ (approximately half of the lattice parameter, i.e $\sim a/2$). Initially, the layers of the wire have A-B-A-B sequence; the atoms of the B-layer face the hallow sites (the center of square unit cell) of the adjacent A-layers. We specify this stacking as the H-site registry. In Fig.5, we illustrate the variation of $\mathbf{F_z}$ as a function of stretch $m\Delta l$, (m, being an integer multiples of increment) and the side views of the structure at the neck region. The $\mathbf{F_z}(m)$ curve displays small fluctuations and also abrupt jumps. The magnitude of the average force increases with increasing m between two consecutive jumps. This is the "quasi" *elastic*

stage[13]. Our results clearly indicate that a new abrupt jump of $\mathbf{F_z}(m)$ occurs whenever approximately $\sim 18-20$ increments are made in an elastic stage following the previous jump. Stated differently, *the tensile force makes a sudden jump and decreases significantly* whenever the length l of the nanowire is elongated by approximately interlayer distance, c. The jump of $\mathbf{F_z}(m)$ starts as the atomic structure of the neck becomes disordered; it lasts until a new layer with relatively smaller crossection is generated. This is the *yielding stage*. The formation of neck layers at fairly regular intervals was predicted earlier[5]. The overall behavior of $\mathbf{F_z}(m)$ is in agreement with the experimental results[3,12,13]. We now examine these in detail.

At the last increment before the first jump in $\mathbf{F_z}(m)$ ($m \sim 19$), the layer structure in the neck is destroyed, and becomes disordered; however it is recovered after a few increments, at $m \sim 24$, with the creation of a new layer (see Fig.5). At the end of this transformation, the crossection of the neck is reduced from 8 atoms to 5 atoms; whereas the crossection of neck layers adjacent to end layers ($n1$ and $n5$) is not altered. The local reduction of the crossection due to stretching causes $|\mathbf{F_z}|$ to reduce, and hence the interlayer spacings between M_3 and $n1$ (and similar spacing at the other end) to decrease. The layer structure of the neck is conserved until $m \simeq 33$. Beyond that point each increment of stretch by Δl causes one atom from the central layer to migrate and stay in the adjacent interlayer spacing which already became wide open due to pulling from $m = 25$ to m =33. This way a new "layer" with two atoms is formed. As a result, the crossection of the connective neck is further reduced with three central layers formed by 5,2,3 atoms, respectively. Owing to the repulsive force induced between the new layer and adjacent ones, $|\mathbf{F_z}|$ decreases abruptly. The asymmetric distribution of atoms in the neck layers may be due to a dynamical effect and due to stretch of the wire from one end, as well. However, in the steps from m=35 to m=38, the asymmetry is lifted by a peculiar, transient event which may be relevant for transport properties: One of the two atoms in the neck layer created at $m = 35$, jumps back to the layer it emerges. During the following increments, the single atom neck is strengthen by the inclusion of one atom from another layer so that the necking becomes uniform by the layers including 4,2,4 atoms. Due to this exchange of atom, the conductance is expected to get a transient dip provided that its duration is long enough. In fact, such a dip has been observed[5]. The two-atom neck becomes stable until the break; but the atoms rotate in the $(xy)-$plane and they become slightly inclined in the z-direction. Such a fluctuation in configuration may give rise to changes in the conductance. It is also seen that the narrowest crossection of the neck prior to the break can have two atoms.

The above results point to the fact that the structural transformations followed by the abrupt change of $\mathbf{F_z}$ result in necking. An additional layer is

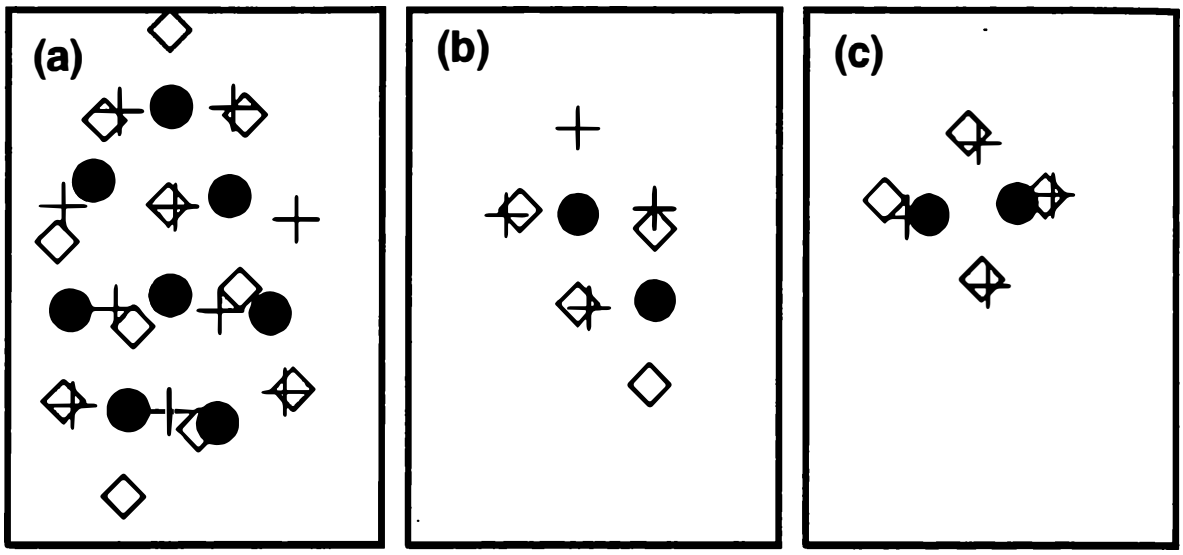

Figure 6. The top view of three layers at the neck showing atomic positions and their relative registry at *three* different levels of stretch. (a) Before the first yielding at $m = 15$ for layers $n2, n3$ and $n4$, with their atomic positions indicated by $+$,$\bullet$ and $\diamond$, respectively. (b) corresponds to $m = 38$, just after the *second* yielding, the structure keeps its registry; while (c) corresponds to $m = 46$, starting the formation of bundle structure. The position of atoms in the *third*, *fourth* and *fifth* layers are indicated by $+$,$\bullet$ and $\diamond$, respectively.

formed and the narrowest crossection decreases usually by more than one atom. In addition to these abrupt changes, we find another mechanism in necking that gives rise to relatively smaller and also slower changes in the crossection. This is a single atom process, in which individual atoms migrate from central layer towards the end layers. The tendency to minimize the surface area and hence to reduce surface energy is the main driving force for this type of necking.

Next we examine atomic rearrangements and structural changes in every atomic layer, which become gradually non-planar under tensile stress. The arrangements of atoms in the layers are shown in Fig.6. In our study we have found that upto $m = 12$, the Cu(001) structure in the neck layers exhibits very small and random deformation (with atomic displacements less than 10% and with no preferable direction), especially those atoms away from the boundary. As shown in Fig.6-(a), the original stacking and registry are kept with least deformation. Beyond a certain stretch, the neck atoms start to built up a structure which deviates from the A-B-A-B stacking sequence of the ideal Cu(001) planes.This deformation starts earlier in the layers $n2, n3$ and $n4$ at $m = 15$. Here we note its two aspects: First, the interatomic distances have slightly increased, especially those of central layers. Second, the $2D$ square lattice changes and then looks like a hexagonal lattice. Upon further elongation of the nanowire, the rest of the neck undergoes the same deformation. The tendency towards a $2D$ hexagonal-like lattice is mediated by the reduced interlayer interaction as a result of

stretch; the atoms try to take relatively low energy configuration in the quasi independent layer behavior. As soon as a new neck layer is formed (at $m \sim 24$), the original features, especially the registry of the Cu(001) layers are recovered at both ends of the neck ($n1$,$n2$ and $n5$,$n6$ layers). These layers (being close to the relatively more stable M_3 and M_4 layers) are forced to return to the original structure. Whereas it is impossible to recover original A-B-A-B sequence of the Cu(001) planes and to match the new layer to the adjacent ones, the incommensurability and deviation from the bulk ordering continues until a new layer is formed. In the present case a new "layer" made of two atoms at the neck is formed at $m \sim 33-35$, but they do not have enough extension to be considered as a real atomic layer. An interesting situation owing to the reduced interlayer interaction and excessive tensile strain appears in the last stage of stretch: The H-site registry disappears eventually shortly before the break and hence the atoms of the adjacent neck layers tend to face the top (T)-sites. This way they are aligned to form atomic chains as shown in Fig.6. As a result, the crystal-like structure and original registry at the neck is replaced by a bundle of atomic chains. In some circumstances, a single atomic chain can form rather than the bundle. Earlier, *ab initio* calculations confirm that the T-site registry is only a local minimum occurring at relatively larger interlayer separation for the Al(111) and Al(001) slabs[28]. However, for some materials oriented in certain atomic planes, the break can take place before such a transition. The transition from the H-site registry to the T-site registry leading to a bundle of chain structure is interesting not only for the point of view of structural modification, but also for novel properties[27,30] (such as "giant" yield strength[12,13] and positive slope of conductance variations[7]).

4.3. MD-RESULTS FOR Cu(111) NANOWIRE

Except for some minor changes, the stretch of nanowire made from Cu(111) layers (as specified by $WN2$ in Fig.4) has overall features of the yielding mechanism at $T = 300K$, which are similar to the above Cu(001) orientation. In Fig.7, we show the force variation with stretch. The force curve depicts consecutive elastic and yielding stages. The elastic stages prior to the first and second structural transformation are rather linear with strain. This is not so in the third stage before the break, where either the structure becomes disordered or changes the registry from the H- to T-site. In fact, after few stretch steps, the magnitude of $\mathbf{F_z}$ drops suddenly due to onset of disorder without formation of a new layer. During the last stage of stretch, the strain is almost accommodated by the layers at the central part of the neck. The $2D$ hexagonal-like structure is quite robust for the layers adjacent or close to the end layers M_3 and M_4. Here the A-B-C stacking sequence

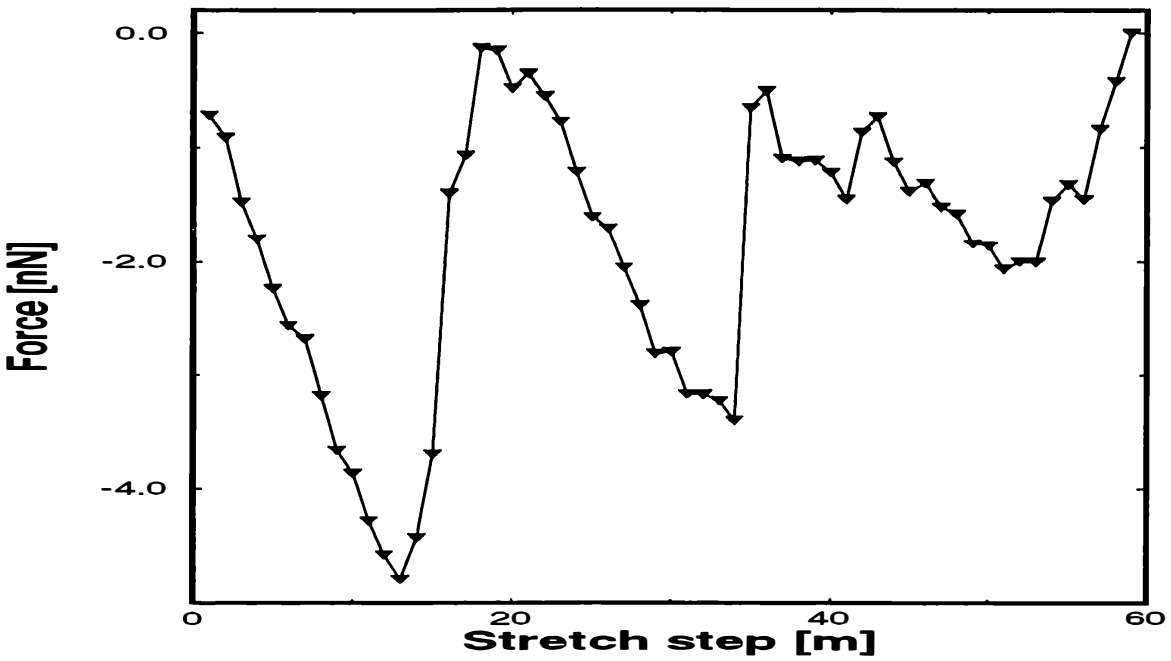

Figure 7. The variation of the tensile force $\mathbf{F}_z$ with the stretch along the z-axis for Cu(001) nanowire ($WN2$) at $T = 300K$.

and the H-site registry are forced by these end layers. In the central part of the neck, the distortion of the $2D$ hexagonal lattice structure becomes severe and the A-B-C sequence disappears, but the H-site registry is kept after the yielding stage. However, the atomic chains form as a result of the transition to the T-site registry in the last stage of stretch.

If the same Cu(111) wire is stretched at low temperature ($T = 150K$), it exhibits features, some of which are dramatically different from those at room temperature. For example, the same wire undergoes *five* yielding stages resulting in an elongation of $9.5\mathring{A}$; whereas at room temperature, it had only *three* yielding steps with $6\mathring{A}$ elongation. Apparently, while the necking is faster and sharper and hence, it is more trumpet-like at room temperature, the neck is longer at low temperature. We explain this with faster atomic motion towards the ends of the wire at room temperature. Another feature which does not exist at room temperature is a new type of structural transformation. The $\mathbf{F_z}(m)$ curve and some relevant side views of the wire in Fig.8 distinguish different types of yielding mechanisms. The first and second yielding stages are similar to the previous cases in which the structure undergoes layer-disordered-layer transformations during the generation of a new layer. At $m = 15$ a well-defined layer structure becomes broader and slightly disordered, and a new layer forms at $m = 16$. This yielding stage occurs more abruptly with least necking; the size of the layers decreases by 2-3 atoms. Similar process repeats at $m = 35$, and creates a new layer at $m = 36$. Again, in this process most of the layers are affected and reduced by two atoms with no significant necking effect. The hexagonal

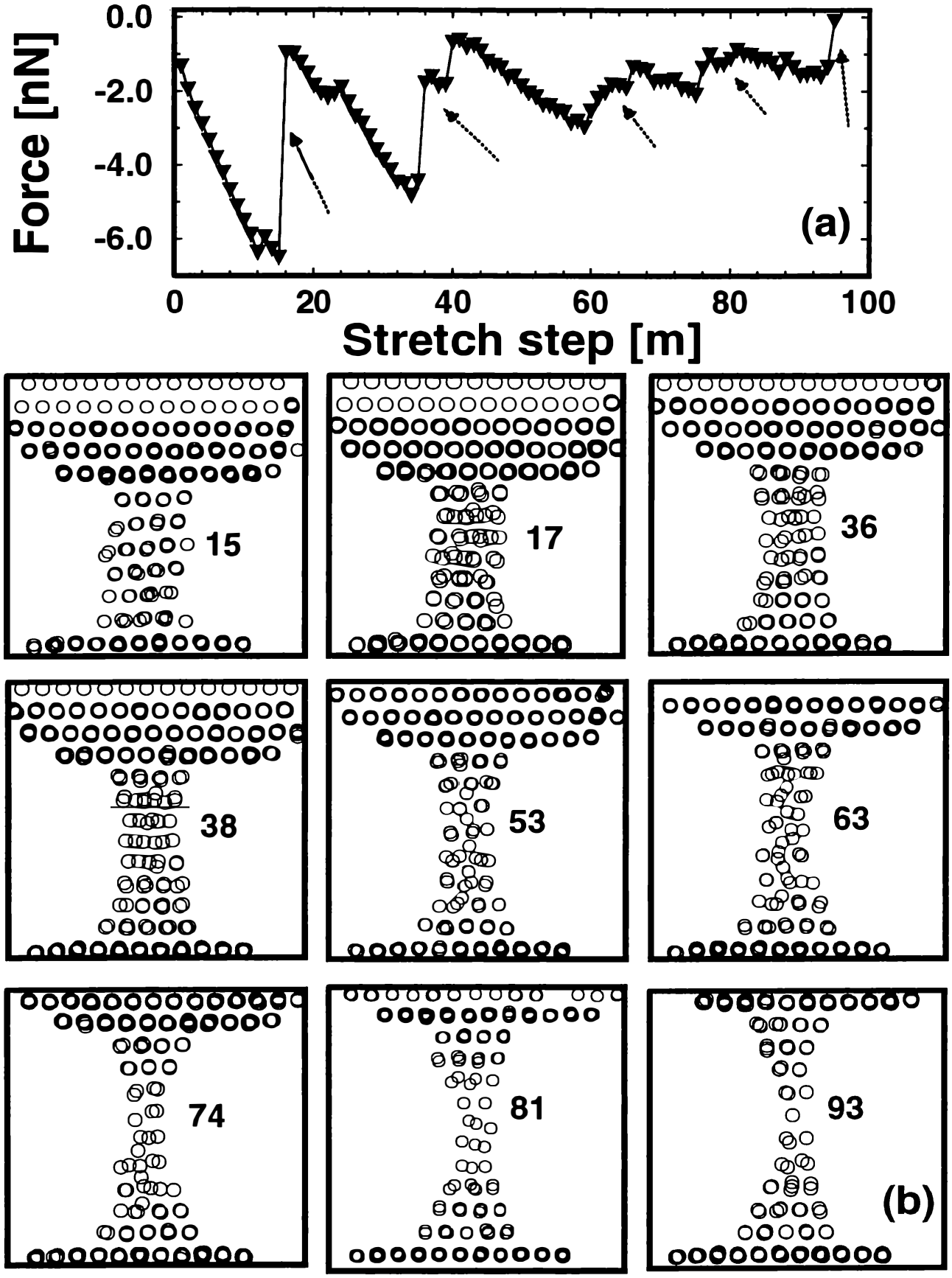

Figure 8. (a) Variation of the tensile Force $\mathbf{F}_z$ with the stretch for the Cu(111) nanowire ($WN2$) at $T = 150K$. We mark the yielding stages by arrows. (b) The side views of the structure at some relevant stretch steps m.

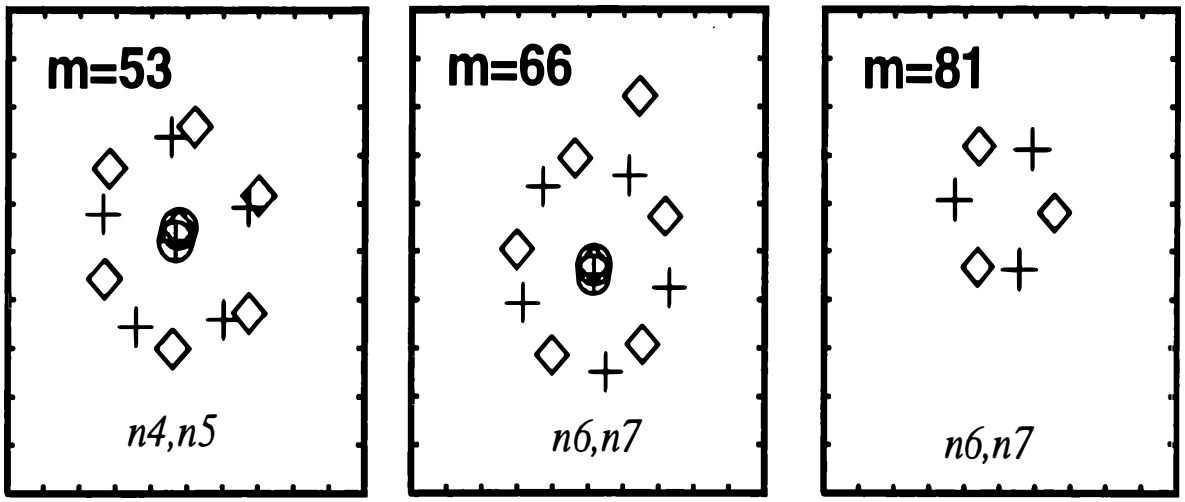

Figure 9. Atomic positions of adjacent layers at the neck center in the (xy)-plane for some relevant stretch steps described in Fig.8. The atoms of the adjacent layers indicated by n's are shown by + and $\diamond$, respectively. The atoms situated in the space above these layers are circled.

rings and A-B-C stacking sequence of the Cu(111) planes are robust near the end layers (M_3 and M_4). At the central layers hexagonal rings persist, but the A-B-C stacking sequence and its characteristic registry between adjacent layers are destroyed. The shape of the layers in the $(xy)-$plane is distorted. For $m > 39$, an intermediate situation occurs within elastic stages: Hexagonal rings change into pentagonal ones; the latter becomes staggered to the rings in the adjacent layers. Moreover, one layer at a time (starting from the central layer) ejects a single atom to the interlayer space. This way a column (or chain) of atoms is formed along the axis of the neck. The projection of this chain in the $(xy)-$plane is almost a single point near the centers of pentagonal rings as shown in Fig.9. Out of *five* yielding stages, the last *three* have this feature. At prolonged stretch ($m > 75$), the number of atoms in the neck layers are reduced and the layer structure becomes more distorted; staggered pentagonal rings change into triangular ones again with staggered orientation. A few steps before break ($84 < m < 94$), a single atomic chain forms eventually. We understand that at low temperatures, the mobility of atoms are not suitable for massive changes, so the neck can accommodate the applied strain by these new intermediate structures which require least atomic rearrangement.

5. Mechanical properties of nanowires

To reveal physical phenomena underlying the "giant" Young's modulus observed in thin wires shortly before the break we carried out *ab initio* calculations by using SCF pseudopotential method within local density approximation. The effective force constant k_{eff}, that is defined as the mechanical force per elongation can be estimated from the slope of the curve $\mathbf{F_z}(m)$. For

a contact, the effective force constant is given by $k_{eff} = R\gamma E/(1-\nu)^2$ (see Ref.12 and 29). Here R, γ, E and ν are respectively contact radius, a factor describing the exact distribution of stress, Young's modulus and Poisson's ratio. From $\mathbf{F_z}$ versus displacement curves measured by the combined STM and AFM, Agraït *et al.*[12] obtained $k_{eff} = 240N/m$ and $R \sim 3nm$. Using the above contact expression of k_{eff}, they estimated $E \sim 66 - 44\ GPa$ which is consistent with the macroscopic value of the Young's modulus of Au. On the other hand, Stalder and Dürig[13] found that the intrinsic yield strength of a neck with $R \sim 1nm$ (corresponding to a crossection $A \sim 300\mathring{A}^2$) between the Au(111) sample and Au tip is 8 GPa, which is one order of magnitude larger than the macroscopic value. This value approached to $20GPa$ shortly before the break. The discussions in the previous section point to the fact that in the last steps of the stretch, where the neck is reduced to $1-3$ atoms, either the bundle of atomic chains or single atomic chain is formed. This structure of the neck is rather different from the original structure derived from the atomic arrangement of the macroscopic bulk and is expected to lead dramatic changes in the mechanical properties. For example, the observed "giant" yield strength may originate from the unusual changes in the structure. By definition, the yield strength σ_Y is the stress, $\sigma = \mathbf{F_z}/A$ at the yield point where the linear relation between stress and strain starts to break. Since $\sigma_Y = E\epsilon_Y$ (ϵ_Y being the strain at the yield point), the observed "giant" yield strength may be due to high strain value and/or high Young's modulus attained by atomic chain. As a matter of fact, owing to the transition from the H-site registry to the T-site registry, a neck can attain large values[28,30] for ϵ_Y. Moreover, *ab initio* calculations that we discuss below demonstrate that E also increases in the neck consisting of atomic chain. Of course, the yield strength and Young's modulus are definitions, which are developed within the continuum description of matter. By adopting some of the variables (such as the crossection A) in these definitions we attempt to calculate E in the quantum limit.

The Young's modulus of an atomic chain can be expressed by $E = kb/A$, where k is the force constant and b is the interatomic distance. Apparently, the size and dimensionality of the chain go beyond the limits of continuum description, and the estimation of k requires *ab initio* quantum mechanical calculations. To this end, we carry out total energy calculations by using SCF pseudopotential method in momentum representation. Accordingly, we take into account the infinite Al-chain whereby we can use periodic boundary condition and pseudopotentials which converge easily for a simple metal. For example, by using the kinetic energy cut-off $|\mathbf{k}+\mathbf{G}| < 7.5Ry$, one can achieve accurate representation of the wave function and band energies. As pointed earlier[28,30], a short Al-chain can form in an Al-neck.

Moreover, the mechanical properties of a short Al-chain can be revealed from those of infinite chain. We use non-local and norm-conserving pseudopotentials[31] with Wigner exchange-correlation potential. We treat the $1D$ infinite atomic chain in a $3D$ supercell geometry in which the interchain distance is taken $7.5\mathring{A}$. The minimum total energy is obtained for $b = 2.403\mathring{A}$. The force constant k is obtained from the variation of total energy relative to interatomic distance b, i.e $k = -\partial^2 E_T(b)/\partial b^2$, and is found $164N/m$. There are ambiguities in the definition of crossection; here we used two schemes which yield similar values: i) $A = 0.38\pi\lambda_F^2$ which is the crossection necessary to open a ballistic conduction channel within free electron and infinite wall cylindrical potential approximation. ii) $A = \pi R^2$; here R is the radius at the value of calculated SCF potential, which is equal to E_F. For Al, we find $A = 15.38\mathring{A}^2$ at $T = 300K$ from the first scheme, and $A \sim 14.0\mathring{A}^2$ from the second scheme. Eventually, we calculate the Young's modulus of Al-chain, $E \sim 260\ GPa$ which is approximately *four* times larger than the bulk value. This implies that the mechanical properties of metal chain or bundle structure is different from those of bulk values, as well as from those of the neck or metal wires having large crossection, such as $A \sim 300\mathring{A}^2$ as in the experiment[13]. The raise of E upon bundle or chain formation may have dominant contribution to the observed "giant" yield strength.

6. Discussion

Our calculations of the conductance for the idealized and circularly symmetric constriction fail to explain the experimental results. In view of this we investigated the effect of the atomic rearrangements induced by the tensile force. Our analysis based on the state of the art molecular dynamics simulations using the embedded atom potential show that the yielding and fracture mechanisms of a nanowire under uniaxial tensile force depend on atomic structure and temperature, and also on the pulling conditions. There are, however, features which are common to all nanowires under uniaxial strain. The important aspects of the present study are summarized:
1. Deformation (or elongation) in two different stages, that occur consecutively and repeat until fracture, are common to all nanowires treated in this study. In the first stage, the stored strain energy and average tensile force increase with increasing stretch, while the layer structure persists. Excluding the fluctuations (possibly due to displacement and relocation of atoms within the same layer or atom exchange between adjacent layers), the variation of $\mathbf{F_z}(m)$ is approximately linear. This stage was identified as elastic. Once the elongation of the nanowire reaches the interlayer separation at the end of the elastic stage, the structure becomes disordered; but after a

few increments of stretch, it is recovered with the formation of a new layer. In this yielding stage, $|\mathbf{F_z}|$ decreases abruptly; the crossection of narrowest neck layers that determines the conductance, in particular the crossection of the layer formed at the end of yielding stage are reduced abruptly by a few atoms. When the neck becomes very narrow (having 3-4 atoms) the yielding is realized, however, by an atom jumping from one of the adjacent layers to interlayer space. On the other hand, it may occur through slips or the motion of dislocations when the wire is much wider. At low temperature, the yielding takes place in relatively shorter time-interval within one or two stretch steps. Owing to the limited mobility of atoms at low temperature, the character of elastic stage changes if the neck is long enough. In this situation, each layer ejects one atom to the adjacent interlayer space as it widens with the applied strain. The layers at the neck are made from the pentagon rings which become staggered in different layers. The interlayer atoms make a chain passing through the center of pentagon rings. In this new phase, the elastic and yielding stages are intermixed and elongation which is more than one interlayer distance can be accommodated.

2. In the initial steps of stretch, the layered structure and ordered $2D$ atomic arrangement within the layers are maintained. Upon increased uniaxial strain (increased m), the layers become wider and rougher due to the atoms departing from the atomic plane, the $2D$ lattice is distorted, and interatomic distances start to deviate from the bulk equilibrium value. In the elastic stage, one can still distinguish layer structure and some kind of order in the atomic arrangement within a layer. In particular, the hallow-site registry between layers are maintained if the layers contain enough number of atoms. The ordered atomic arrangement becomes disordered at low temperature towards the end of stretch.

3. The elastic and following yielding stages are reminiscent of the stick-slip motion. In the course of stretch, elastic and yielding stages repeat; the surface of the nanowire roughens and deviates strongly from circular symmetry. The narrowest part, which is only a layer thick, is connected to horn-like ends. Our results of atomic simulations point to the fact that neither adiabatic evolution of discrete electronic states, nor circular symmetry induced degeneracy can occur in the neck. Consequently any quantized sharp structure shall be smeared out by channel mixing and tunneling[9]. On the other hand, owing to the sudden reduction of crossection by a few atoms, some states contributiong to current carrying states are eliminated suddenly. This leads to sudden drop of G with stretch as described by dashed line in Fig3-b.

4. In addition to the stick-slip behavior under strain, atoms also migrate in a much slower process. The migration process speeds up with increasing temperature and its effect on necking becomes significant when a thin neck

has a canonical connection to the ends. Also a transient and permanent exchange of atoms between adjacent layers can take place. This may lead to transient dips on spikes in the $G(s)$ curve.

5. If the interlayer interaction is reduced as a result of extensive strain the $2D$ atomic structure (square-like lattice) is transformed into hexagonal rings. At prolonged stretch, just before the the break, the crossection of layers at the central part of the neck is reduced to $2-3$ atoms. In this case, the H-site registry may change to the T-site registry. This leads to the formation of bundle of atomic chains or single atomic chain. We consider this a dramatic change in the atomic structure of the wire and may have important implications. The positive slope of $G(s)$ curve at the last plateau of Al can be explained by the chain formation[30].

6. Our *ab initio* calculations of Young's modulus on the $1D$ metal chains indicate that the neck having chain structure may have yield strength much higher than the bulk value. This is in good agreement with experimental results[3,12,13], and also implies that the elastic properties of an atomic size neck deviate from those of the bulk defined in the continuum limit.

In conclusion, the simulations of atomic structure in nanowires under tensile stress indicate novel mechanisms of plastic deformation and elongation. When the restoring effect of the initial structure is weakened under the applied uniaxial force, the atomic arrangement deviate from the global minimum and can be stabilized in a different local minimum. The corresponding configuration exhibits a non-crystalline, short-range order and interesting mechanical and transport properties induced thereform.

Acknowledgements

We would like to thank Prof. M. S. Daw for providing embedded atom potential for Cu and Dr. E. Tekman, Prof. Ş. Erkoç and Dr. B. Tanatar for helpful discussions.

References

1. For extensive review see:(1991) J.L. Beeby(eds.), *Condensed Systems of Low Dimensionality*, NATO ASI Series B, Phys. Vol. **253**, Plenum Press; (1991) L. Esaki(eds.), *Highlights in Condensed Matter Physics and Future Prospects*, NATO ASI Series B, Phys. Vol. **285**, Plenum Press.
2. Gimzewski, J.K. and Möller, R. (1987) Transition From the Tunneling Regime to Point Contact Studied by Scanning Tunneling Microscopy, *Phys. Rev. B***36**, 1284-1287.
3. Landman, U., Luedtke, W. D., Burnham, N. A. and Colton, R. J. (1990) Atomistic Mechanisms and Dynamics of Adhesion, Nanoindentation and Fracture, *Science* **248**, 454-461.
4. Agraït, N., Rodrigo, J. G. and Vieiria, S. (1993) Conductance Steps and Quantization in Atomic-Sized Contacts, *Phys. Rev. B***47**, 12345-12348.

5. Pascual, J. I., Mèndez, J. , Gòmez-Herrero, J., Barò, A. M., Garcia, N. and Binh, V. T. (1993) Quantum Contact in Gold Nanostructures by Scanning Tunneling Microscopy, *Phys. Rev. Lett.* **71**, 1852-1855; Pascual, J.I., Mèndez, J., Gòmez-Herrero, J., Barò, A. M., Garcia, N., Landman, U., Luedtke, W.D., Bogachek, E.N. and Cheng H.P.(1995), Properties of Metallic Nanowires: From Conductance Quantization to Localization, *Science* **267**, 1793-1795.
6. Olesen, L. , Laegsgaard, E., Stensgaard, I., Besenbacher, F., Schiøtz, J., Stoltze, P., Jacobsen, K.W. and Nørskov, J. K. (1994) Quantization Conductance in an Atom-sized Point Contact, *Phys. Rev. Lett.* **72**, 2251-2254; (1995) Olesen et al. Reply, *Phys. Rev. Lett.* **74**, 2147-2147.
7. Krans, J.M., Müller, C.J., Yanson, I.K., Gowaert, Th.C.M., Hesper R. and Ruitenbeek, J.M. (1993) One Atom Point Contact, *Phys. Rev. B***48**, 14721-14724.
8. Ciraci, S. and Tekman, E. (1989) Theory of Transition from the Tunneling Regime to Point Contact in Scanning Tunneling Microscopy, *Phys. Rev. B***40**, 11969-11972; Ciraci, S. (1990) Tip Surface Interactions, in R.J. Behm, N. Garcia and H. Rohrer(eds.), *Scanning Tunneling Microscopy and Related Methods*, Kluwer Academic Publishers, Volume **184**, pp.113-141.
9. Tekman, E. and Ciraci, S. (1991) Theoretical Study of Transport through a Quantum Point Contact, *Phys. Rev. B***43**, 7145-7169.
10. Todorov, T.N. and Sutton, A.P. (1993) Jumps in Electronic Conductance due to Mechanical Instabilities, *Phys. Rev. Lett.* **70**, 2138-2141.
11. Krans, J.M. Müller, C.J., Van der Post, N., Postama, F.R., Sutton, A.P., Todorov, T.N. and Ruitenbeek, J.M. (9995) Comments on Quantized Conductance in an Atom-sized Point Contact, *Phys. Rev. Lett.* **74**, 2146-2146.
12. Agraït, N., Rubio, G and Vieiria, S. (1995) Plastic Deformation of Nanometer-Scale Gold Connective Necks, *Phys. Rev. Lett.* **74**, 3995-3998; Rubio, G., Agraït, N. and Vieiria, S. (1996) Atomic-sized Metallic Contacts, *Phys. Rev. Lett.* **76**, 2302-2305.
13. Stalder, A. and Dürig, U. (1996) Study of Yielding Mechanics in Nanometer-sized Au Contacts, *App. Phys. Lett.* **68**, 637-639.
14. Landauer, R. (1957) Spatial Variation of Currents and Fields due to Localized scatterers in Metallic Conduction, *IBM J. Res. Develop.***1**, 223-231.
15. Sharvin, Yu.V. (1965) A Possible Method for Studying Fermi Surfaces, *Zh. Eksp. Teor. Fiz.* **48**, 984-985; [*Sov. Phys.-JETP* **21**, 655-656].
16. Van Wees, B.J., Van Houten, H., Beenakker, C.W.J., Williamson, J.G, Kouwenhoven, L.P., van der Marel, D. and Foxon, C.T.(1988) Quantized Conductance of Point Contacts in a Two-Dimebsional Electron Gas, *Phys. Rev. Lett.* **60**, 848-850.
17. Wharam, D.A., Thorton, T.J., Newbury, R., Pepper, M., Ahmed, M., Frost, J.E.F, Peacock, D.G., Ritchie, D. A. and Jones, G.A.C. (1988) One-Dimensional Transport and the Quantization of the Ballistic Regime, *J. Phys. C***21**, L209-L214.
18. Büttiker, M., Imry, Y., Landauer, R. and Pinhas, S. (1985) Generalized Many Channel Conductance Formula with Application to Small Rings, *Phys. Rev. B***31**, 6207-6215; Imry, Y. (1986) Physics of Mesoscopic Systems, in G. Grinstein and G. Mazenko(eds.), *Directions in Condensed matter Physics*,World Scientific Publisher, Singapore, pp.101-163.
19. Beenakker, C.W.J and van Houten, H. (1991) Quantum Transport in Semiconductor Nanostructure, in H. Ehrenreich and D. Turnbull(eds.), *Solid State Phys.***44**, Academic Press,Inc., pp.1-170.
20. Lang, N.D. (1987) Resistance of a One-Atom Contact in the Scanning Tunneling Microscope, *Phys. Rev. B***36**, 8173-8176.
21. Ferrer, J., Martin-Rodero, A. and Flores, F. (1988) Contact Resistance in the Scaaning Tunneling Microscope at very small Distances, *Phys. Rev. B***38**, 10113-10115.
22. Daw, M.S. and Baskes, M.I. (1984) Embedded-atom Method: Derivation and Application to Impurities, Surfaces and Other Defects in Metals, *Phys. Rev. B***29**, 6443-6453.

23. Foiles, S.M., Baskes, M.I. and Daw, M.S. (1986) Embedded-atom Method functions for the FCC Metals Cu, Ag, Au, Ni, Pd, Pt and their Alloys, *Phys. Rev. B***33**, 7983-7991.
24. Daw, M.S. (1989) Model of Metallic Cohesion: The Embedded-atom Method, *Phys. Rev. B***39**, 7441-7452.
25. Lynden-bell, R.M. (1994) Computer Simulations of Fracture at the atomic level, *Science* **263**, 1704-1705.
26. Bratkovsky, A.M, Sutton, A.P. and Todorov, T.N. (1995) Conditions for Conductance Quantization in Realistic Models of Atomic-scale Metallic Contacts, *Phys. Rev. B***52**, 5036-5051.
27. Mehrez, H., Ciraci, S. and Erkoç, Ş. (1997) Yielding and Fracture Mechanisms of Nanowires, *Phys. Rev. B* (to be published).
28. Ciraci, S., Baratoff, A. and Batra, I.P. (1990) Site-dependent Electronic Effects, Forces and Deformation in Scanning Tunneling Microscopy, *Phys Rev. B***42**, 7618-7621, for Al(111) surface; and Ciraci, S., Tekman, E., Baratoff, A. and Batra I.P. (1992) Theoretical Study of Short- and Long- Range Forces and Atom Transfer in Scanning Tunneling Microscopy, *Phys. Rev. B***46**, 10411-10422, for Al(001) surface.
29. Johnson, K.L. (1986) *Contact Mechanics*, Cambridge University Press, Cambridge.
30. Mehrez, H., Ciraci, S., Buldum, A. and Batra, I.P. (1997) Conductance through a Single Atom, *Phys. Rev B***55**.
31. Bachelet, G.B., Hamann, D.R. and Schlüter, M. (1982) Pseudopotentials that work from H to Pu, *Phys. Rev. B***26**, 4199-4228.